ORNL/SPR-2023/3248

FWP FEAA149: "Next Generation Environmental Barrier Coatings"

M. J. Ridley
B. A. Pint

December 2023

OAK RIDGE NATIONAL LABORATORY
MANAGED BY UT-BATTELLE FOR THE US DEPARTMENT OF ENERGY

U.S. Department of Energy
Fossil Energy and Carbon Management Materials Final Program Report

FWP FEAA149: "NEXT GENERATION ENVIRONMENTAL BARRIER COATINGS"

M. J. Ridley, B. A. Pint

End Date of Reporting Period: 9/30/2023

Prepared by
OAK RIDGE NATIONAL LABORATORY
Oak Ridge, TN 37831
managed by
UT-BATTELLE LLC
for the
US DEPARTMENT OF ENERGY
under contract DE-AC05-00OR22725

SUMMARY

Environmental barrier coatings (EBCs) are required coatings for utilization of SiC/SiC ceramic matrix composite (CMC) components in gas turbines, where the EBC represents the life-limiting factor for such components. EBC/CMC systems have shown success in aero-engine applications with increased turbine inlet temperatures and improved efficiencies, which are achieved through higher temperature stability, lower density, and decreased reliance on cooling air compared to traditional superalloys. While industrial gas turbines (IGTs) do not currently utilize SiC/SiC CMCs, the current shift towards low-carbon or carbon-free fuel sources for power generation could result in a need for EBC/CMC components with higher temperature capabilities. In this work, three tasks were outlined to improve understanding of EBC lifetimes to encourage use in IGTs with carbon-free fuel such as hydrogen: 1. Define the bond coating oxidation kinetics and EBC failure criteria, 2. Measure thermal expansion coefficients of each layered material, and 3. Perform advanced characterization and modeling to assess EBC lifetimes. Cyclic steam oxidation tests were conducted on various EBC/Si/SiC chemistries and EBC/SiC architectures to define substrate oxidation kinetics and EBC failure modes. An open-source code was developed to quantify the undulating thermally grown oxide thickness with thousands of measurements from specimen cross-section images. Bond coating oxidation kinetics were determined and used to develop a kinetic and thermodynamic model for predicting EBC lifetimes. High-temperature Raman spectroscopy was utilized for determining the SiO_2 thermally grown oxide phase transformation as the life-limiting feature for EBCs. Model efforts supported the claim that the SiO_2 phase transformation causes elevated stress during thermal cycling with associated cracking that decreases the adhesion strength of the EBC, eventually resulting in coating spallation. The finite element model subroutine will be made publicly available upon internal review. Further development of an EBC lifetime model for IGTs involves definition of a critical SiO_2 thickness for EBC spallation and must also consider both environmental (gas velocity, pressure, etc.) and specimen (EBC dopants, layer architectures, etc.) effects into predicted bond coating oxidation kinetics for long-lifetime components.

MILESTONE REPORT

Milestone Designation	Milestone Description	Completion Date
ORNL-149-1	Measure reaction kinetics in flowing air-steam environments at ≥3 temperatures and 2 times with and without a Si bond coating	6/2020
ORNL-149-2	Measure the mean thermal expansion of monolithic specimens of at least two substrate-coating components	12/2019
ORNL-149-3	Define a maximum CMC temperature for ≥25,000 h EBC operation and compare assumptions to data available in the literature	9/2020
ORNL 149-4	Complete thermal expansion measurement task by measuring values for at least two ceramic materials to ≥1200°C	3/2021
ORNL 149-5	Conduct EBC durability testing at ≥1350°C in air-steam environments for at least 1,500 1-hr cycles or until failure	12/2020
ORNL 149-6	Further refine the lifetime predictions for maximum CMC temperature for ≥25,000 h EBC operation based on new data inputs	8/2021
ORNL 149-7	Submit a journal publication on studying thermally grown silica and EBC phase composition using Raman spectroscopy	6/2022
ORNL 149-8	Compare the cyclic oxidation performance and scale growth rate in air- 90%H2O of two EBC-coated SiC substrate roughnesses at two temperatures	3/2022
ORNL 149-9	Compare the silica growth rate and cyclic oxidation durability of Yb disilicate and mixed Y-Yb disilicate EBC coatings with and without a Si bond coating	6/2022
ORNL 149-10	Calibrate Raman Si peak shift as a method to quantify stress associated with silica phase transformation and explore the effects of water vapor and scale thickness on stress	6/2023
ORNL 149-11	Predict the average stress associated with the silica phase transformation as a function of silica thickness and compare to the thermal expansion mismatch stress	10/2022
ORNL 149-12	Evaluate two modified EBC/bond coating compositions in air-water cyclic testing and compare the scale growth rates at three temperatures to baseline EBC performance	7/2023

1. INTRODUCTION

SiC/SiC ceramic matrix composites (CMCs) have shown success for implementation into aero turbines as hot-section components to replace Ni-base superalloys. The resulting high-temperature chemical stability, high-temperature strength, and reduced density of CMCs show promise for large reductions in greenhouse emissions during fuel burn through increased operating temperatures and reduced cooling. SiC CMCs are known to degrade in the presence of H_2O, a byproduct of fuel combustion, thus necessitating the addition of environmental barrier coatings (EBCs) to minimize oxidation and mitigate oxide volatilization in exhaust gas.

EBCs are a required technology for use of CMCs in turbines and are hence the focus of this work at ORNL regarding industrial gas turbines (IGTs). Inclusion of CMC/EBC components into IGTs may eventually be necessary as worldwide efforts are placed towards low carbon or carbon-free fuel sources to replace natural gas. For example, hydrogen or blend of hydrogen and natural gas fuels show promise for utilization in next-generation IGTs. However, the combustion temperature of hydrogen can be higher than that of natural gas to achieve similar power output. In addition, the combustion of hydrogen will result in an increased H_2O partial pressure in the combustion gas, resulting in a more corrosive high-temperature environment. EBC/CMC systems are likely required to withstand this more aggressive environment, and in addition, efficiency gains from such components could offset the high costs associated with hydrogen production, transport, and storage.

ORNL research efforts focused on EBC development, testing, and advanced characterization to develop a lifetime model that would lower barriers for implementation of EBC/CMC systems into IGTs with hydrogen-base fuel sources. Steam oxidation reaction kinetics were assessed in a variety of test cases for multiple EBC chemistries and architectures. Fundamental material properties were measured to support the development of a model and general understanding. In tandem, advanced characterization was employed to generate a comprehensive understanding of performance and primary degradation modes, which can be fed into the EBC lifetime model. The primary three tasks of this project were:

Task 1: Define bond coating oxidation reaction kinetics and failure criteria

Task 2: Measure thermal expansion coefficients of each layered material

Task 3: Perform advanced characterization and modeling

Summaries of each task efforts are presented below. This work involved multiple collaborations that greatly furthered the research presented here. Coating fabrication was conducted at Stony Brook University (SBU) on CVD SiC specimens and focused on state-of-the-art Yb silicate top coatings with and without a Si bond coating. Dense monolithic specimens were fabricated through a collaboration with the University of Virginia for thermal expansion measurements. Additional specimens were obtained from two industrial partners and a collaboration with NASA Glenn Research Center (GRC). Ongoing discussions with NETL, Arizona State University, and Tennessee Tech University are focused on future collaborative efforts to address knowledge gaps remaining in the EBC lifetime and durability model development.

2. TASK 1: DEFINE BOND COATING OXIDATION REACTION KINETICS AND FAILURE CRITERIA

Furnace cycle testing (FCT) were conducted in steam/air mixtures using 1-h cycles in automated cyclic oxidation rigs. Because the specimens are only coated on one side and both oxidation and evaporation processes are occurring, values of specimen mass change are not especially useful to determine the kinetics of these processes. Therefore, silica thermally grown oxide (TGO) kinetics on the Si bond coatings under EBCs were quantified by measuring the reaction product thickness as a function of time using a specially developed image analysis algorithm applied to images obtained using metallographic cross-sections. SOFIA, size of oxidation feature image analysis, is a code developed through this project for measuring layer thicknesses based on greyscale separation from specimen characterization images [1]. This code was made publicly available for external use via GitHub (*https://github.com/TriplePointCat/SOFIA-CV*). Long term cyclic exposures were conducted to identify failure mechanisms at 1250°, 1300°, 1350°, and 1425°C. Land based turbines for power generation are expected to undergo longer cycle times at elevated temperatures compared to aero turbine cycles. The baseline research standard EBC system (Figure 1) was utilized for most of the testing to serve as a baseline for comparison to more novel EBC chemistries and architectures.

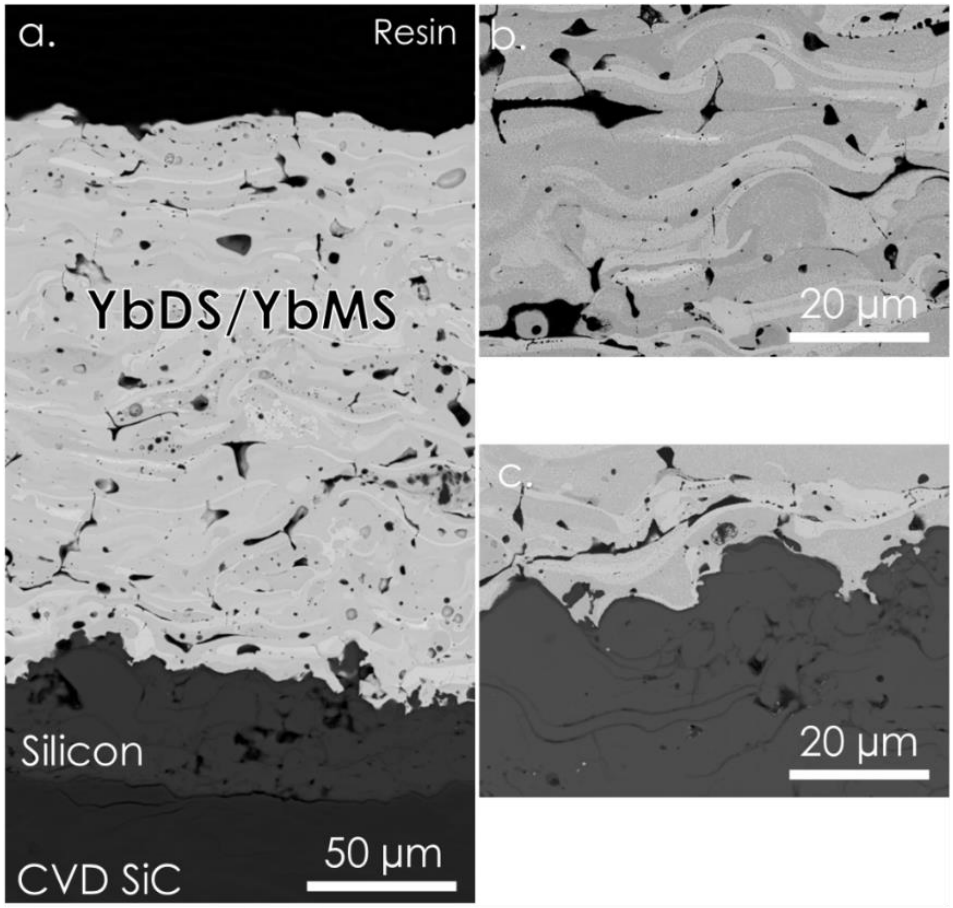

Figure 1. Cross-section backscattered electron (BSE) scanning electron microscope (SEM) images of YbDS/YbMS EBC after 4 h anneal at 1300°C in stagnant laboratory air, a. full EBC/Si cross-section, b. high-magnification of the EBC, and c. high-magnification of the Si-EBC interface.

Initial baseline oxidation data were collected for uncoated SiC and Si coupons at 1250°-1350°C [2, 3]. The resulting oxide thicknesses were measured and parabolic reaction rates were determined. An Arrhenius plot in Figure 2 shows the temperature dependence for each substrate in both air and steam environments. Steam oxidation showed over an order of magnitude increase in oxidation rate for both SiC and Si, with temperature dependences comparable to values reported in the literature. The goal for EBC development is to produce a protective EBC such that a specimen could be exposed to steam yet show reduced order oxidation kinetics similar to the air exposure environment.

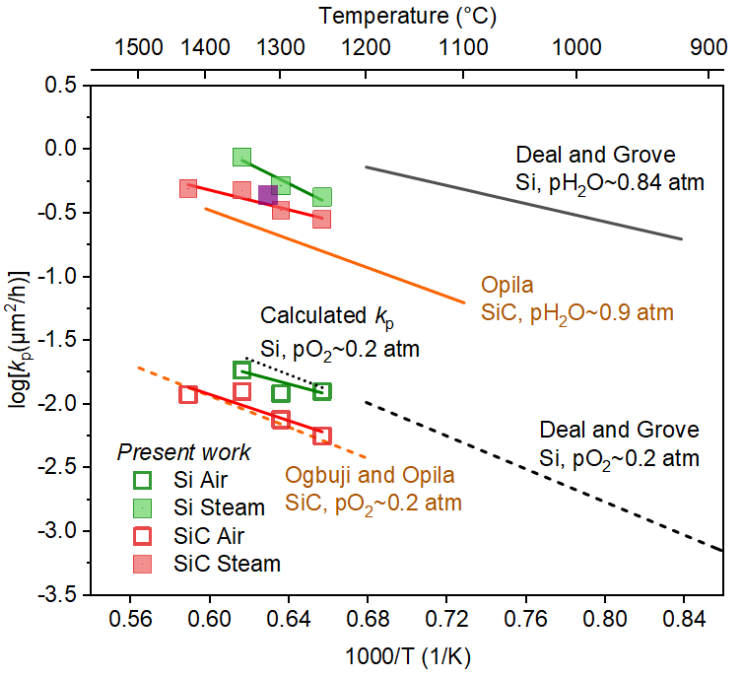

Figure 2. Arrhenius plot of uncoated SiC and Si oxidation.

Sample geometry limitations, such as an EBC deposited on only one sample face, can result in edge delamination artifacts that limit total testing times to the order of 1000 h. Single sided EBC coupons, which are standard for R&D efforts, also show edge spallation of coating and oxide at sharp edges, resulting in the mass loss shown in Figure 3a for EBC coupons with and without a Si bond coating [2]. The cross-section of YbDS/YbMS EBC with a Si bond coating after exposure to 1350°C 1000 h (Figure 3b) shows the delamination of the EBC at specimen edges, indicating localized EBC failure.

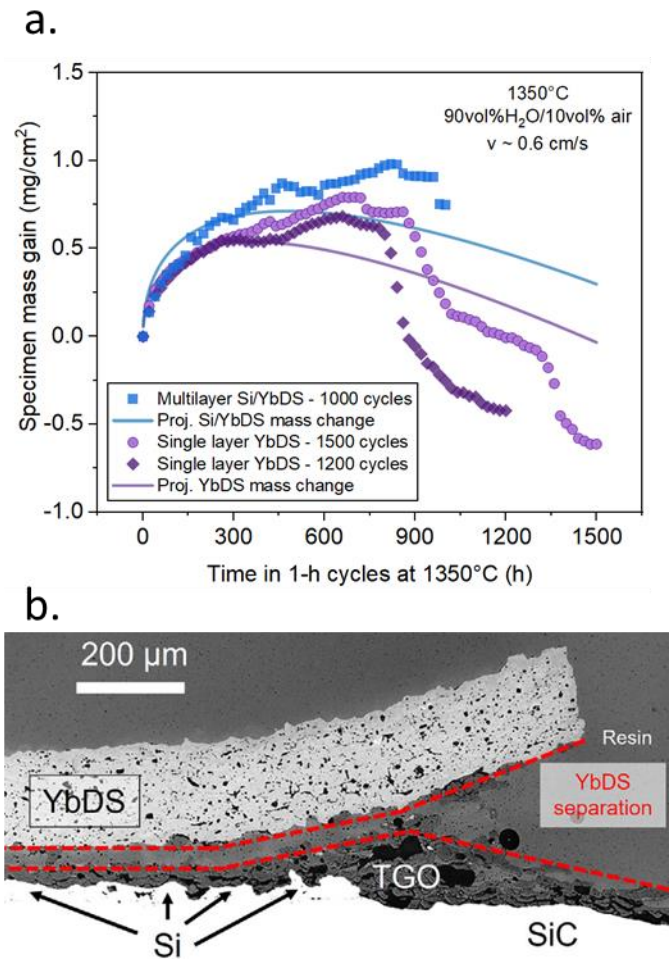

Figure 3. a. Specimen mass change during 1-h thermal cycles with and without a Si bond coating, b. YbDS/YbMS EBC with Si bond coating after 1000 cycles at 1350°C showcasing EBC delamination and failure as specimen edges.

A commercial mixed rare earth EBC chemistry from an industrial partner, (Y/Yb)DS or $(Y_{0.6}Yb_{0.4})_2Si_2O_7$, was compared against the research standard EBC chemistry of YbDS/YbMS ($Yb_2Si_2O_7/Yb_2SiO_5$) at 1350°C to determine performance, Figure 4. Clear improvements were found with the Y-containing EBC, where the oxide thickness was suppressed under the same test conditions. Pore development was also evident in the (Y/Yb)DS, which is not desirable long term.

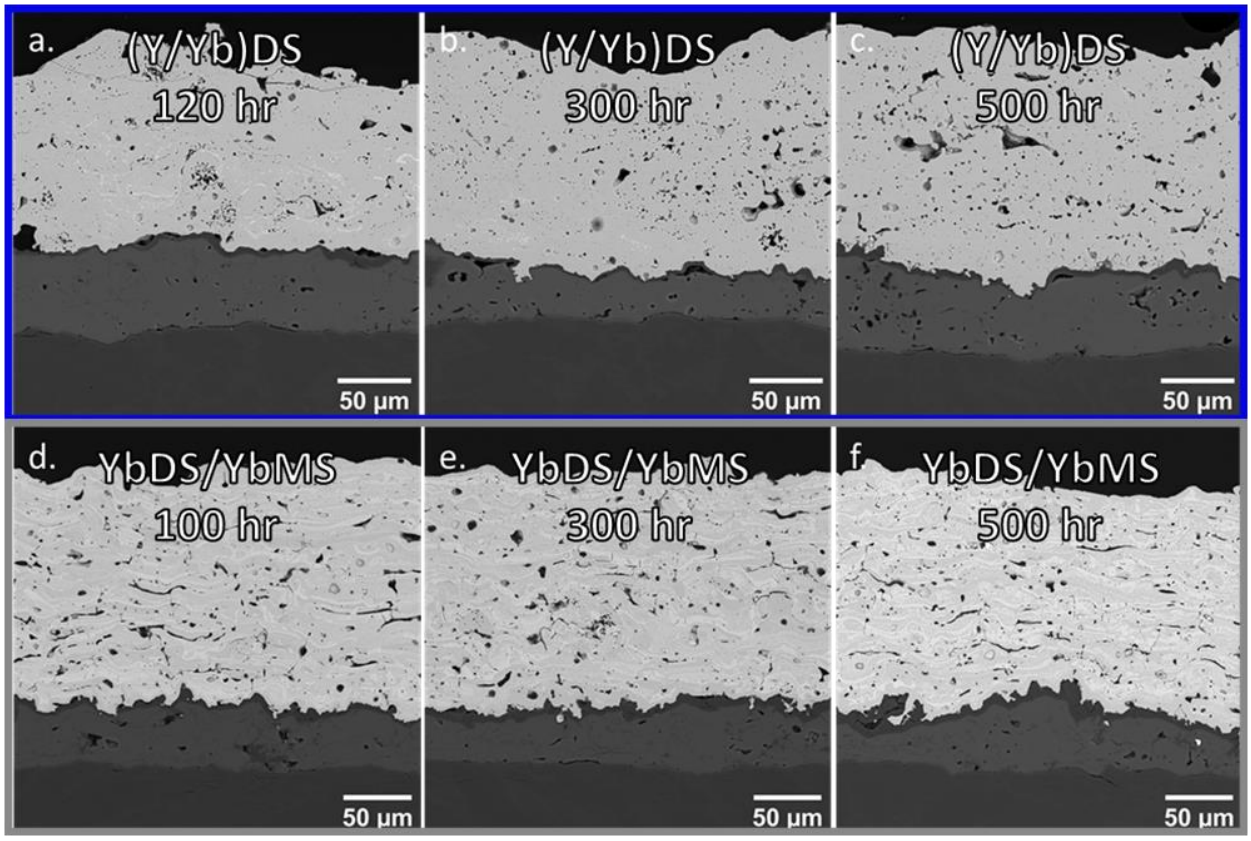

Figure 4. Steam oxidation of a., b., c. (Y/Yb)DS and d., e., f. YbDS/YbMS up to 500 1-h cycles.

An Arrhenius plot in Figure 5 shows the EBC performance relative to both Si and SiC oxidation in air and steam [4, 5]. Initial temperature dependence data for YbDS/YbMS EBCs with and without a Si bond coating has also been published [3]. It is clear that EBC systems in the air environment outperform all other test conditions, as this is a less aggressive test gas compared to 90% H_2O (g). (Y/Yb)DS EBCs outperformed the YbDS/YbMS EBCs in both air and steam thermal cycle testing, where the (Y/Yb)DS in 1-h steam cycles performed similarly to uncoated Si in air. Yet, 100-h cycles of the (Y/Yb)DS showed greater pore growth in the coating, which ultimately changed the reaction kinetics. Both sets of coatings – (Y/Yb)DS and YbDS/YbMS – were manufactured with two different suppliers, and therefore comparison is challenging. Further work is needed to fully understand the effect of composition on performance.

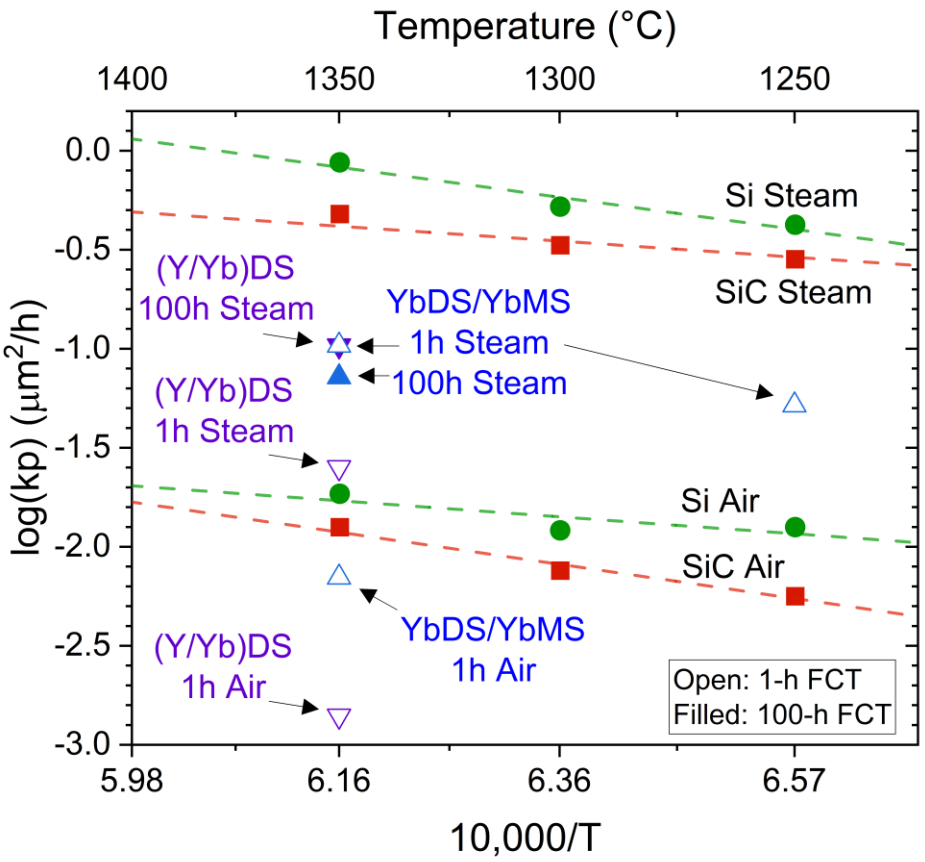

Figure 5. Arrhenius temperature dependence of EBC systems in both air and steam environments.

For the model, the kinetic data at 1350°C were extrapolated both in time and temperature space for the YbDS/YbMS EBC system to create a visualization of TGO layer thickness for extended use in IGTs, Figure 6. The color scale corresponds to predicted SiO_2 TGO thicknesses. Extrapolations were verified through comparison of other experimental data at 1250°C and 700°C, shown in Table 1. Excellent agreement was found between the calculated and experimental SiO_2 thicknesses. It is unclear if initial formation of a SiO_2 scale is amorphous or crystalline in the β-cristobalite phase, and such differences may impact oxidant transport and subsequent growth rates. Additionally, it is believed that the initial scale thickness may play a more dominant role when extrapolating down in temperature space, where very thin scales are present. Increased statistics may be required to appropriately assess TGO thicknesses for lower temperature exposures.

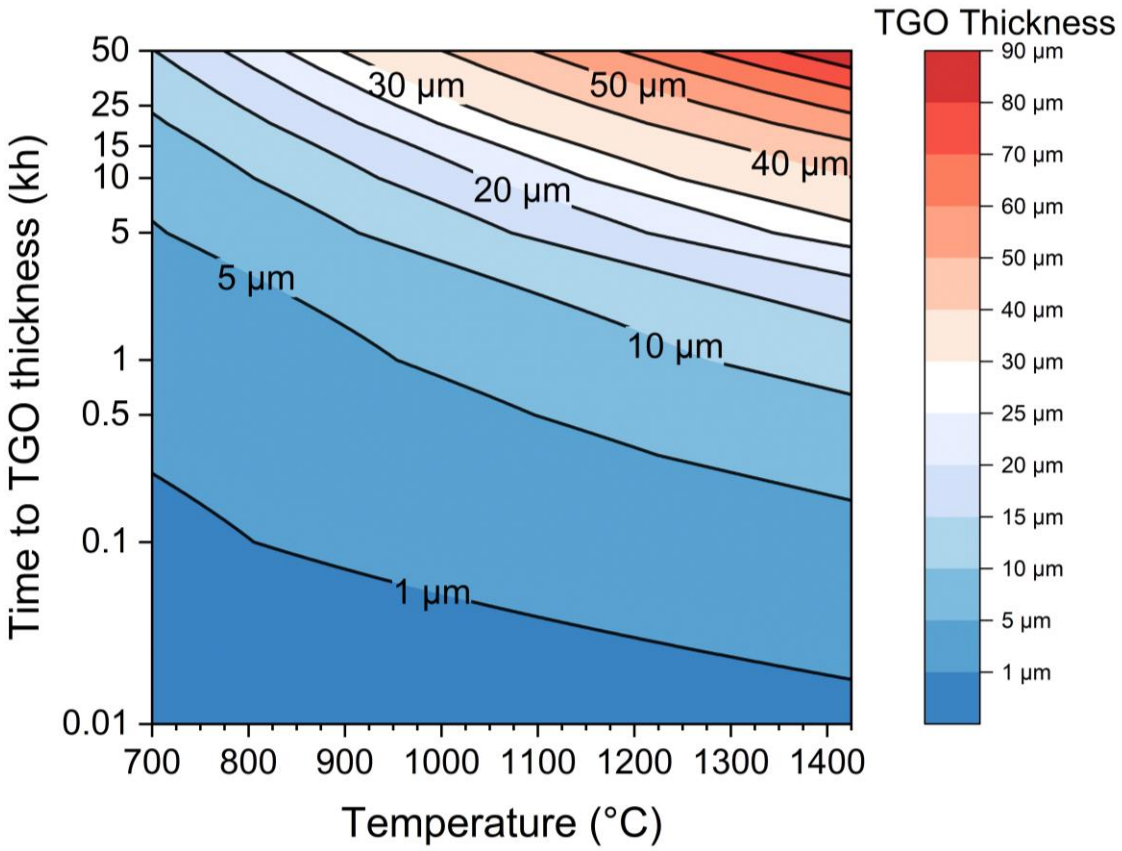

Figure 6. Kinetic model for oxidation of the Si bond coating under a 200 µm YbDS/YbMS EBC based on 1.5 cm/s flow of 90% H_2O (g) / 10% air with 1-h thermal cycling.

Table 1. Model validation to other test data. Measured data are average SiO_2 thickness.

Time (h)	1350°C		1250°C	
	Model	**Measured**	**Model**	**Measured**
100	3.53	3.40	3.00	3.15
300	6.12	6.15	5.19	5.19
500	7.90	7.90	6.70	6.69
k_p ($\mu m^2/h$)	0.125	0.125	0.090	0.087

Multiple architectures were explored to assess the lifetime of EBC/SiC systems without a Si bond coating, as the Si melts at 1414°C and limits the upper use temperature of EBC systems. Enhanced roughness SiC substrates were constructed via laser engraving. The various enhanced roughness SiC types are presented on Figure 7, which include typical a monolithic CVD SiC substrate that is grit blasted and two different enhanced roughness levels, R1 and R2.

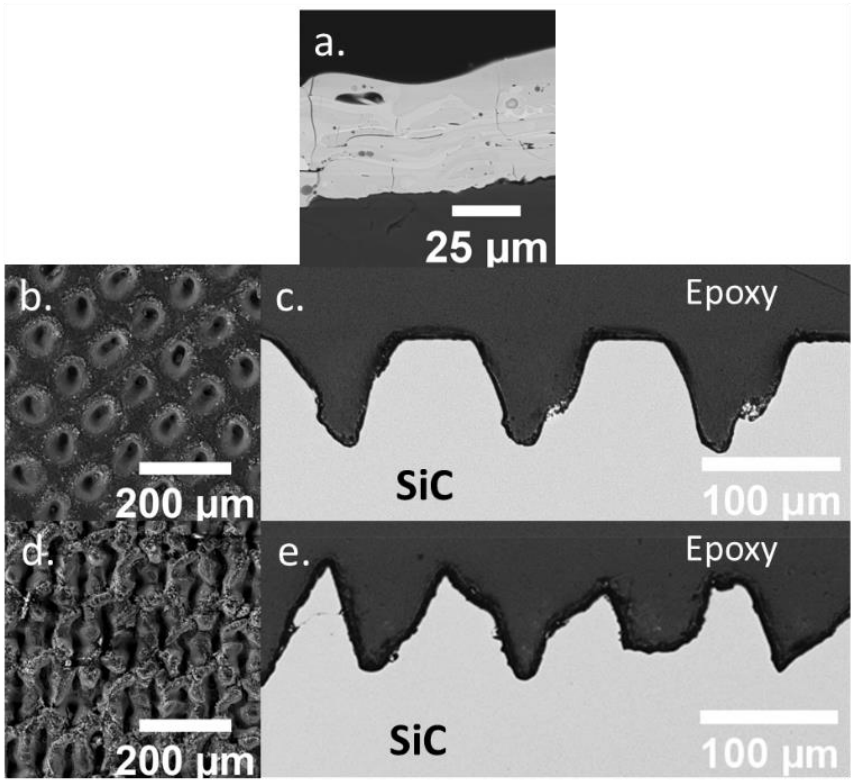

Figure 7. a. Grit blasted SiC with a 60 µm EBC topcoat, b. R1 SiC surface, c. R1v2 SiC cross-section, d. R2 SiC surface, and e. R2 SiC cross-section.

Both 60 and 200 µm thick EBCs were deposited directly on grit blasted SiC for steam cycling exposures. Before experimentation, the 200 µm EBCs delaminated from the substrates, preventing testing due to the lack of chemical bonding to the substrates. Coating delamination occurred relatively fast for all exposure conditions. Figure 8a shows the TGO thickness after 280 1-h cycles at 1250°C where the EBC had spalled, and from Figure 8b delamination had occurred after less than 50 cycles at 1350°C [6].

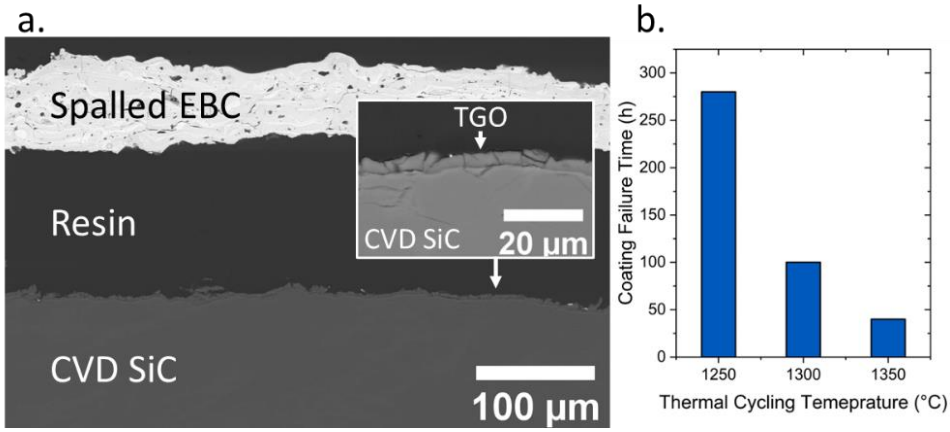

Figure 8. a. Grit Blasted SiC with 60 µm EBC topcoat after 280 1-h FCT at 1250°C, b. EBC delamination time as a function of thermal cycling temperature.

Samples with the two laser roughened surfaces are compared in Figure 9 after thermal cycling at 1350°C in flowing steam for 500 h. A green dashed line is overlaid at the SiC-SiO_2 interface for clarity, due to the similar greyscale from SEM imaging. Similar characteristics are found between 60 µm EBC (Figure 9a) and 180 µm EBC (Figure 9b) on R1 substrates; the SiO_2 TGO thickness was designated into flat and concave regions with similar performance. The 180 um YbDS/YbMS EBC on R2 (Figure 9c) showed much more aggressive oxidation [7]. Finally, a 220 um (Y/Yb)DS EBC on R2 SiC (Figure 9d) showed a high variability in TGO thickness, and also showed signs of crack development in the EBC through pore and crack coalescence between the engraved SiC grooves. The oxidation kinetics of each architecture are shown on Figure 10. The 60 µm and 180 µm YbDS/YbMS EBCs on R1 SiC showed similar oxidation kinetics, yet the 60 µm EBC showed a higher median SiO_2 thickness due to the shorter oxidant diffusion distance through the EBC. The thickest EBC tested in this exploratory study, 220 µm (Y/Yb)DS on R2 SiC, showed both the lowest parabolic oxidation rate but also a rapid transition to linear kinetics by 500h, indicating EBC delamination would soon occur due to rapidly crossing a critical TGO thickness threshold for EBC delamination. YbDS/YbMS on R2 SiC also showed linear oxidation kinetics.

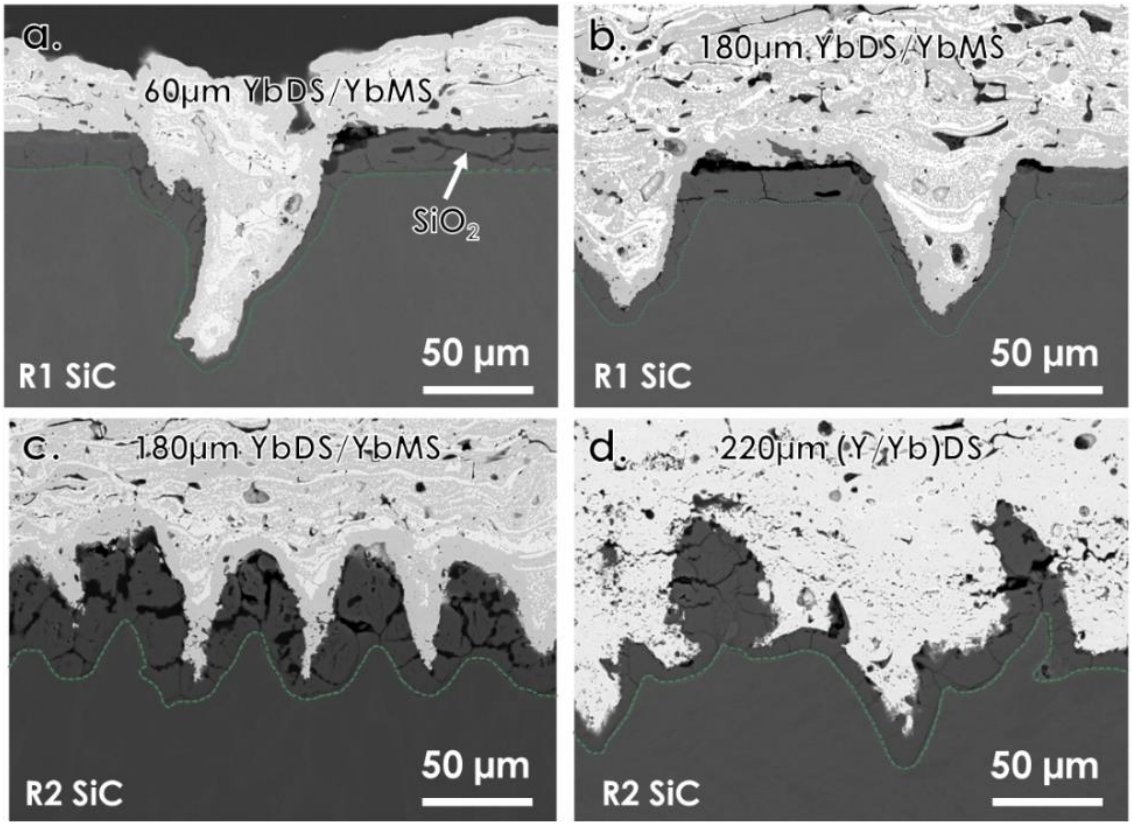

Figure 9. Cross-section SEM images showing the SiO_2 scale morphology after 1350°C and 500h cyclic steam exposure for a. 60 um YbDS/YbMS EBC on R1 SiC, b. 180 um YbDS/YbMS EBC on R1 SiC, c. 180 um YbDS/YbMS EBC on R2 SiC, and d. 220 um (Y/Yb)DS EBC on R2 SiC.

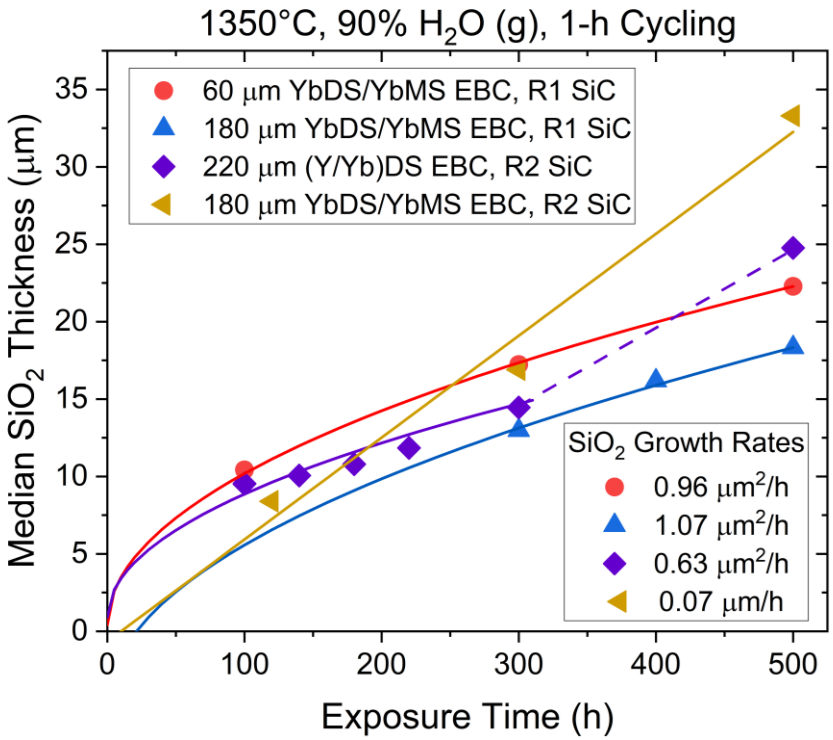

Figure 10. Comparison of median SiO_2 thicknesses for various EBC chemistries, thicknesses, and SiC roughness architectures after cyclic steam exposures at 1350°C.

The impact of EBC chemistry was compared in Figure 11 with cross-section SEM images after 100 1-h cycles at three temperatures. Here, YbDS/YbMS EBCs were compared to (Y/Yb)DS EBC on roughened SiC (no Si bond coating) and two doped EBC samples after 100 hours of cyclic steam exposure at 1250, 1300, and 1350°C. The scale bars are unique for each system, to best showcase performance. The SiO_2 scale thickness increased with increasing temperature as expected. Complete removal of the Si bond coating and enhanced roughness of the SiC substrate did not result in promising performance in laboratory testing. While improved understanding of oxidation mechanisms was learned, no further work is planned with EBCs without a bond coating. In order to increase the maximum operating temperature above the melting temperature of Si, either a larger temperature gradient is needed across the EBC to achieve a lower temperature for the Si bond coating or new bond coating compositions are needed. Both doped EBC systems shown displayed nonuniform thermally grown oxide scales which were not measurable at 1250 and 1300°C. Longer exposure times are needed to quantify performance of doped EBCs at these temperatures

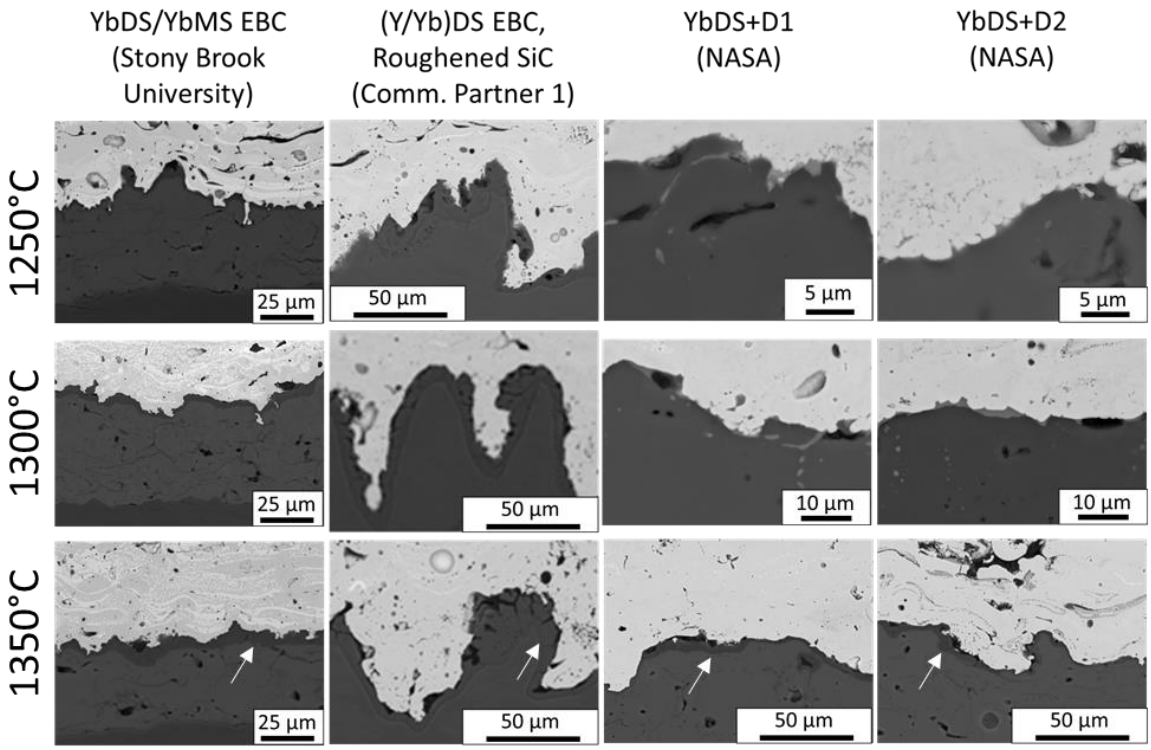

Figure 11. Cross-section SEM images of EBC systems after exposure to 1250, 1300, and 1350°C steam cycling for 100h. D1 and D2 represent dopant additions. White arrow indicates SiO_2 TGO.

3. TASK 2: MEASURE THERMAL EXPANSION COEFFICIENTS

Coefficient of thermal expansion (CTE) measurements were performed on processed dense bulk materials to provide the model data about CTE mismatch among the coating layers [8]. During the project, a new dilatometer was acquired at ORNL that allowed CTE measurements to 1500°C. Minimal differences in CTE were measured between CVD SiC and the metallic Si bond coating. It is clear that $Yb_2Si_2O_7$ (YbDS) is a better match with SiC/Si compared to the higher CTE of Yb_2SiO_5 (YbMS). YbDS showed some degree of deformation above 1400°C, indicative of thermal creep or sintering behavior under the slight compressive load of the pushrod dilatometer. The thermal expansion of fused silica was negligible compared to the other layer properties. Such properties will be utilized in the EBC thermal stress model, discussed later in Task 3.

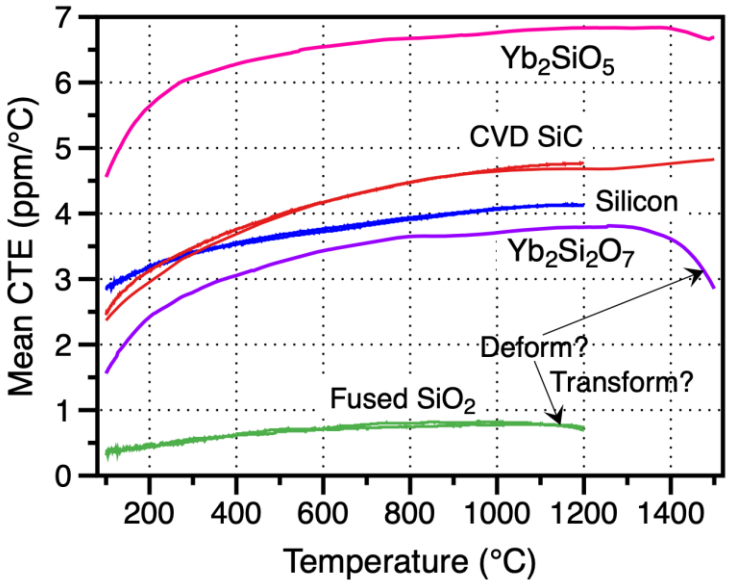

Figure 12. Thermal expansion coefficients of monolithic layers within the EBC/CMC system architecture.

Rather than dense sintered monolithic materials, Figure 12 shows the CTE measurement repeated on thermally sprayed compositions: C1 60% YbDS/40% YbDS and C2 90% YbDS/10% YbMS [7]. The thermal spray process results in an initially amorphous coating, where upon heating a volume decrease was observed around 1000°C-1200°C, which corresponds to crystallization. Utilizing these data, the crystallization heat treatments utilized for EBC testing at ORNL (1300°C for 4h in air) was verified. After crystallization the cooling curves for both C1 and C2 show more uniform behavior. Additional dilatometric cycles, not shown, result in repeatable CTE values as the initial cycle cooling curve.

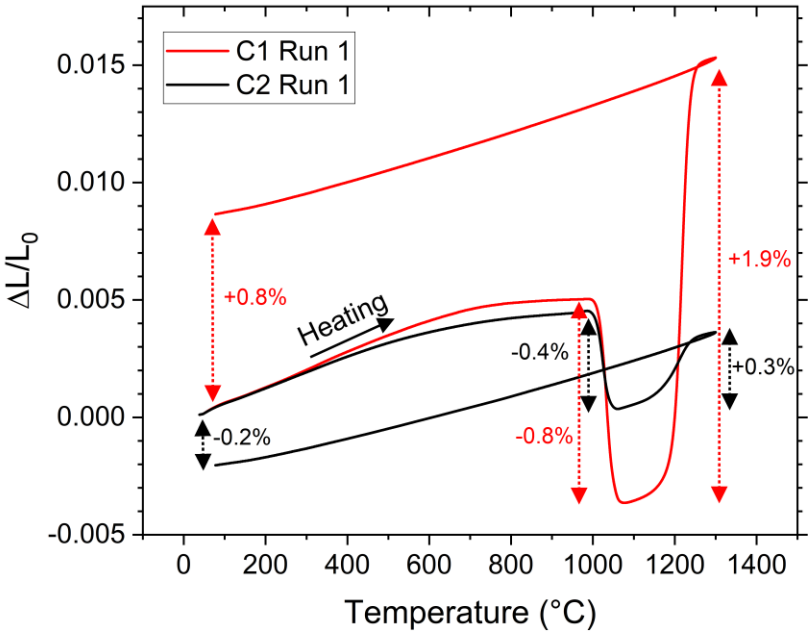

Figure 13. YbDS/YbMS compositions (C1 and C2) dilatometer length changes upon phase stabilization and crystallization.

4. TASK 3: PERFORM ADVANCED CHARACTERIZATION AND MODELING

This task helped to achieve a better mechanistic understanding of the relevant reactions at high temperature in Task 1 through characterization and model development. Effects on oxidation behavior can be subtle (but important in determining life) and often may require advanced or high-resolution microscopy techniques to reveal the root causes of changes in scale growth rates or coating failure mechanisms that might suggest possible routes to improved coating performance. The results from Tasks 1 and 2 were used to construct an IGT-relevant EBC lifetime model. Of particular interest was: 1. the estimated maximum CMC temperature, 2. the required temperature gradient based on the model output, and 3. The stress magnitudes and energy release rates from cycling EBCs with various SiO_2 TGO interfaces.

EBC finite element modelling was used in the initial development stages. It has been shown through Task 2 that the CTE of the EBC is pertinent information for determining the thermal stresses upon cycling. Further, there is a SiO_2 (cristobalite) crystallographic phase transformation that occurs around 250°C. This phase change results in ~5% volume change with ~30 times change in the CTE value. As such, the stress magnitudes of the thermal stress and SiO_2 transformation stress were compared to determine what has the greatest impact on TGO crack formation and propagation. Resulting modelling efforts were supported through Raman spectroscopy of SiO_2 scales from room temperature up above the transition temperature for the cristobalite phase change.

The initial finite element modelling of the EBC/Si/SiC system was performed with Abaqus software. For the model, CTE's measured at ORNL and CTE of the silica TGO from the literature were used as inputs. Additionally, temperature dependent moduli and Poisson's ratios were included. The model consisted of three primary test regions. First, the system was considered at zero stress at 1300°C and was cooled to the silica phase transformation temperature of 250°C. This step represents the primary thermal stress. Then, the phase change was modelled, and the stresses were recalculated. Finally, the system was cooled to room temperature to determine the total stress upon cooling. Results were calculated as a function of TGO thickness of 0, 5, 15, and 30 µm (Figure 14). Three unique architectural systems were explored, shown in Figure 15. Implementation of material density and volume changes are not directly available with standard finite element modelling code. As such, a UMAT (User Material) subroutine was developed to incorporate the SiO_2 volume change that occurs when the phase transformation is underway around 250°C. This UMAT was demonstrated on simplified code for verification and has now been implemented into the original FEM mesh for calculation of stresses upon temperature cycling with various TGO thicknesses.

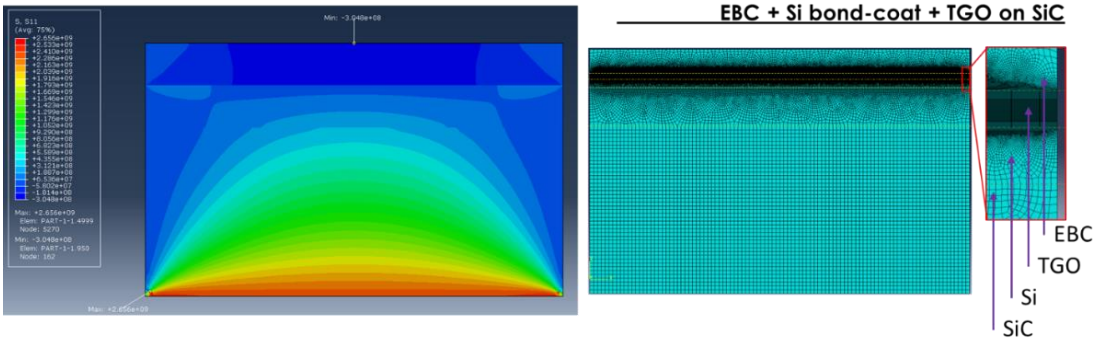

Figure 14. Representative stress model and calculation nodes for the EBC/TGO/Si/SiC system. In the right image, the mesh appears black at the TGO interface due to a large increase in node density to provide higher model accuracy.

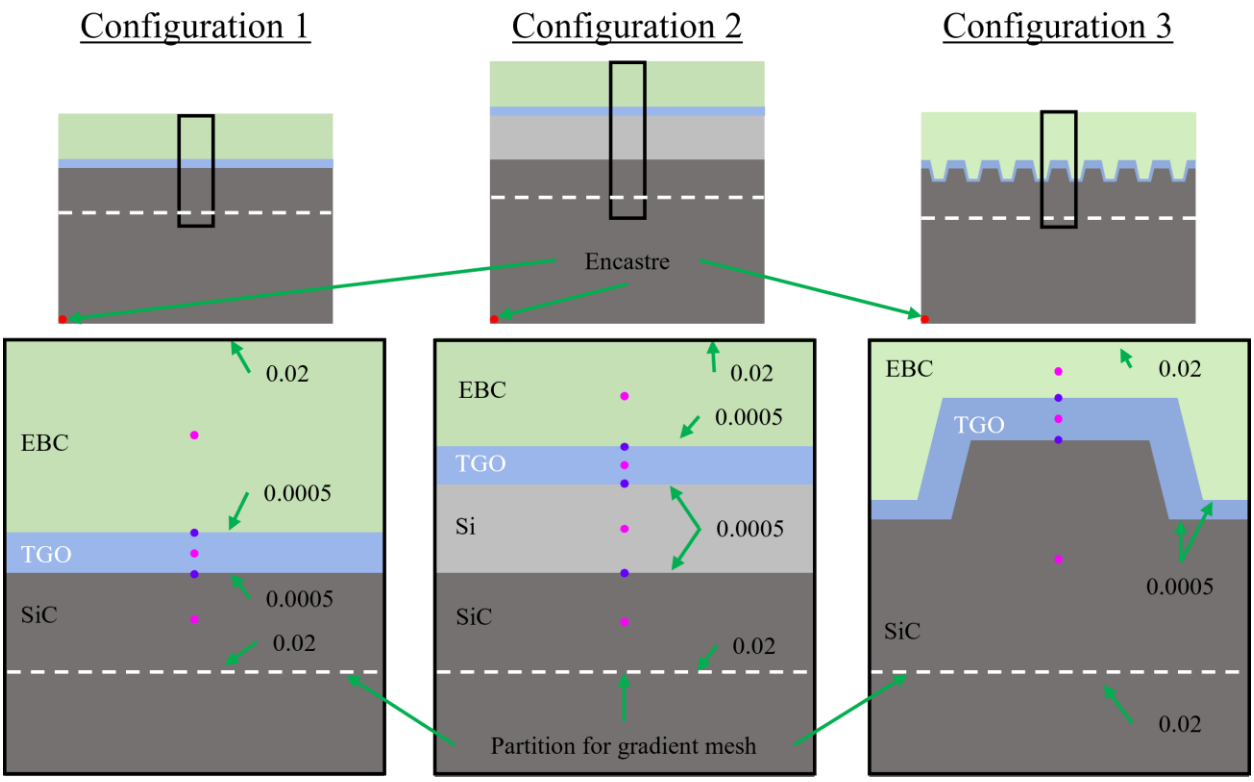

Figure 15. Schematic for FEM Configurations 1, 2, and 3. The bottom row displays the material sections, data collection locations, and mesh seed size at each interface from each panel in the top row. The magenta dots indicate where the data were collected from in the bulk material and the purple dots indicate where data were collected from at the interfaces. The red dot indicates the node that had the encastre boundary condition.

For the SiO_2 TGO – EBC interface, the maximum and minimum principal stresses were calculated for each configuration at the EBC – TGO interface, shown in Figure 16. During the initial cooling stage from 1350°C to 251°C (thermal stress only), the interface experiences compressive stresses near ~200 MPa for all configurations. Thermal stresses are shown to be independent of SiO_2 TGO thickness. Upon TGO phase transformation at 250°C, a very large tensile stress on the order of 1.6 GPa dominated the system stresses for all system configurations. The present figure highlights the detrimental effect of the SiO_2 phase transformation on the EBC lifetime, as this high-stress event is expected to control interfacial cracking and eventual coating delamination. The present data is representative of an idealized system where the TGO has no defects. Accounting for microstructural defects should provide a more realistic stress analysis of the system and can be related to crack density measurements from furnace cycle tests. After internal review, the UMAT will be made publicly available for utilization outside of ORNL.

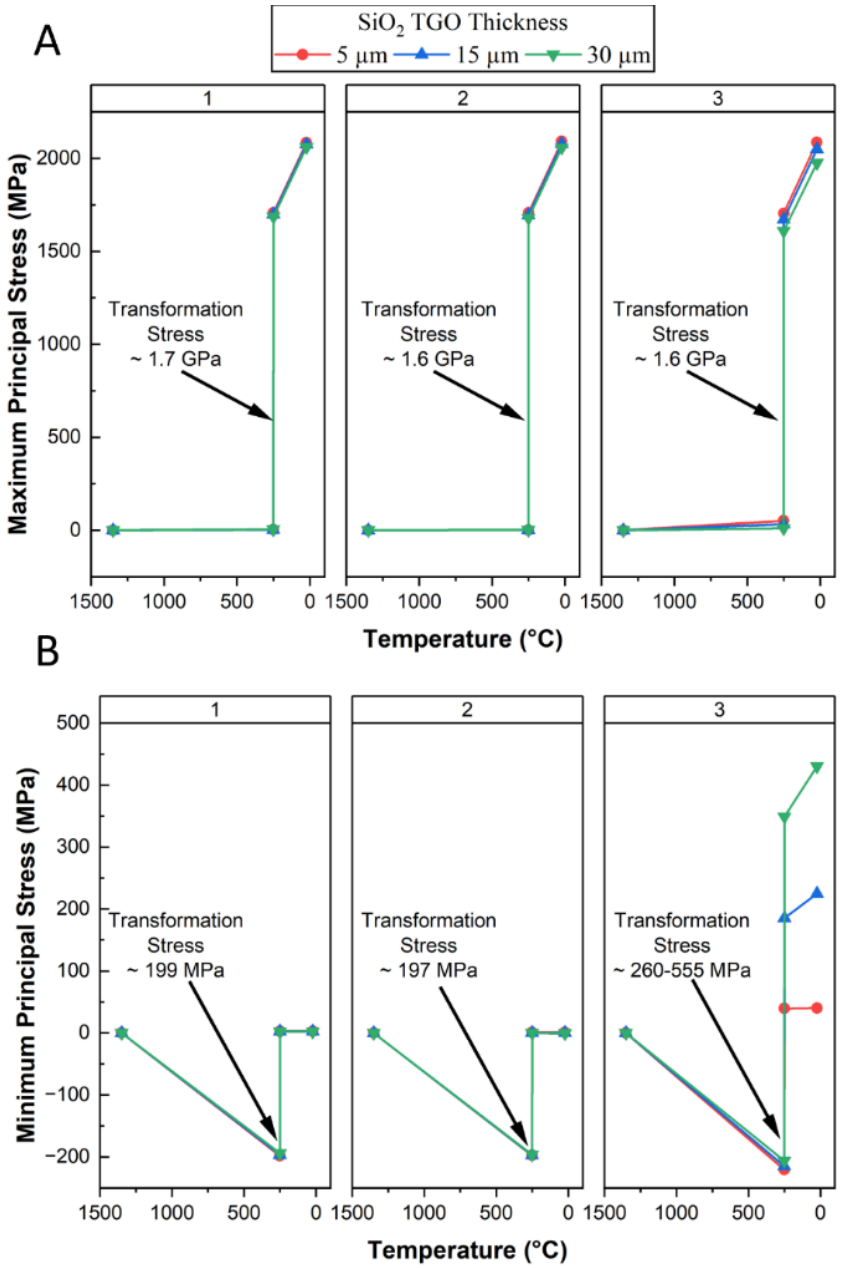

Figure 16. TGO a. Maximum Principal and b. Minimum Principal Stresses for Configurations 1, 2, and 3. The number at the top of each panel indicates which Configuration the data are from.

Raman spectroscopy was initially utilized as a characterization tool strictly for tracking phase evolution at room temperature. Major progress was made on development of calibration standards, data analysis techniques, and complex testing capabilities to improve the capabilities of Raman spectroscopy for EBC characterization. Figure 17 shows initial room temperature Raman spectroscopy maps of YbDS/Si/SiC system after the crystallization anneal before testing and after 500 1-h thermal cycles at 1250°C. Each phase was identified based on Raman spectra with a raster stage to generate a phase map. It was confirmed that the silica thermally grown oxide was crystalline cristobalite phase.

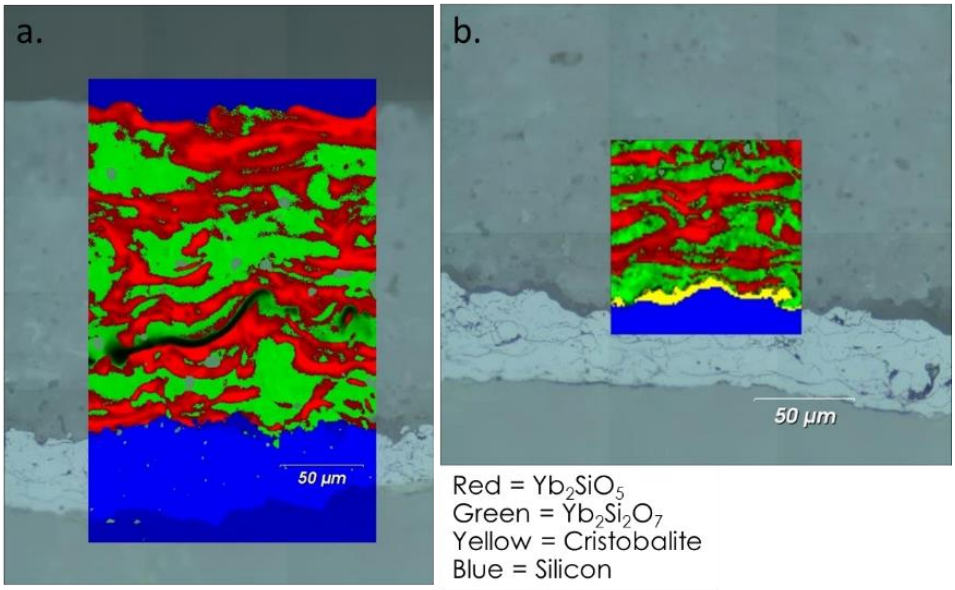

Figure 17. Room temperature Raman spectroscopy mapping of YbDS/YbMS EBC system a. after crystallization anneal, and b. after 500 1-h steam cycling at 1250°C.

Calibrations were performed for peak shifting of Si to quantify stress states during temperature exposures. The peak shift as a function of applied stress was measured with a micro tensile stage. A linear shift in Si peak position was measured at -3.39×10^{-4} cm^{-1}/MPa for uniaxial stress. The present Si peak shift results agree with the expected value of ~4×10^{-4} cm^{-1}/MPa. Figure 18 shows the temperature evolution of electronics grade Si after exposure to steam at 1350°C for 100h. The alpha cristobalite SiO_2 peaks can be seen up until the silica phase transformation. Further optical imaging shows how initially present cracks in the silica were closed due to the 5% volume increase upon heating through the phase transformation. Biaxial stresses were calculated, using bare Si as a reference Raman peak position. The resulting analysis showed that the stress associated with the silica phase transformation without an EBC topcoat was on the order of 400 MPa [9].

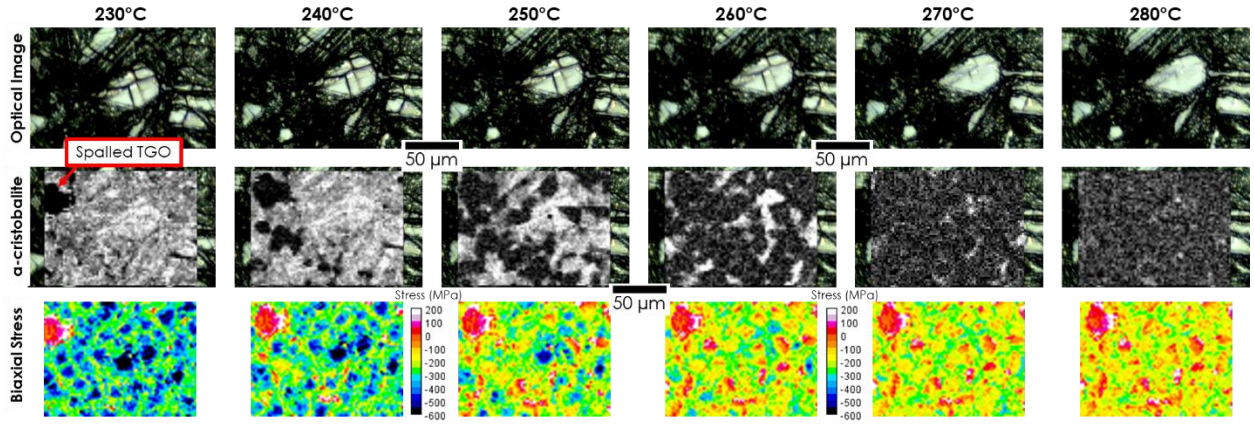

Figure 18. Raman characterization SiO_2 phase transformation after exposure of an electronics grade Si wafer at 1350°C for 100h.

Figure 19a highlights the cross-section of an EBC/Si bond coating/SiC system after exposure to flowing 90% steam at 1350°C for ten 100-h cycles. The optical image shows the thick cracked SiO_2 TGO of interest. Figure 19(b, c, d) show the average Raman spectra and the Raman phase maps at both 260°C before the phase transformation and at 270°C after the phase transformation.

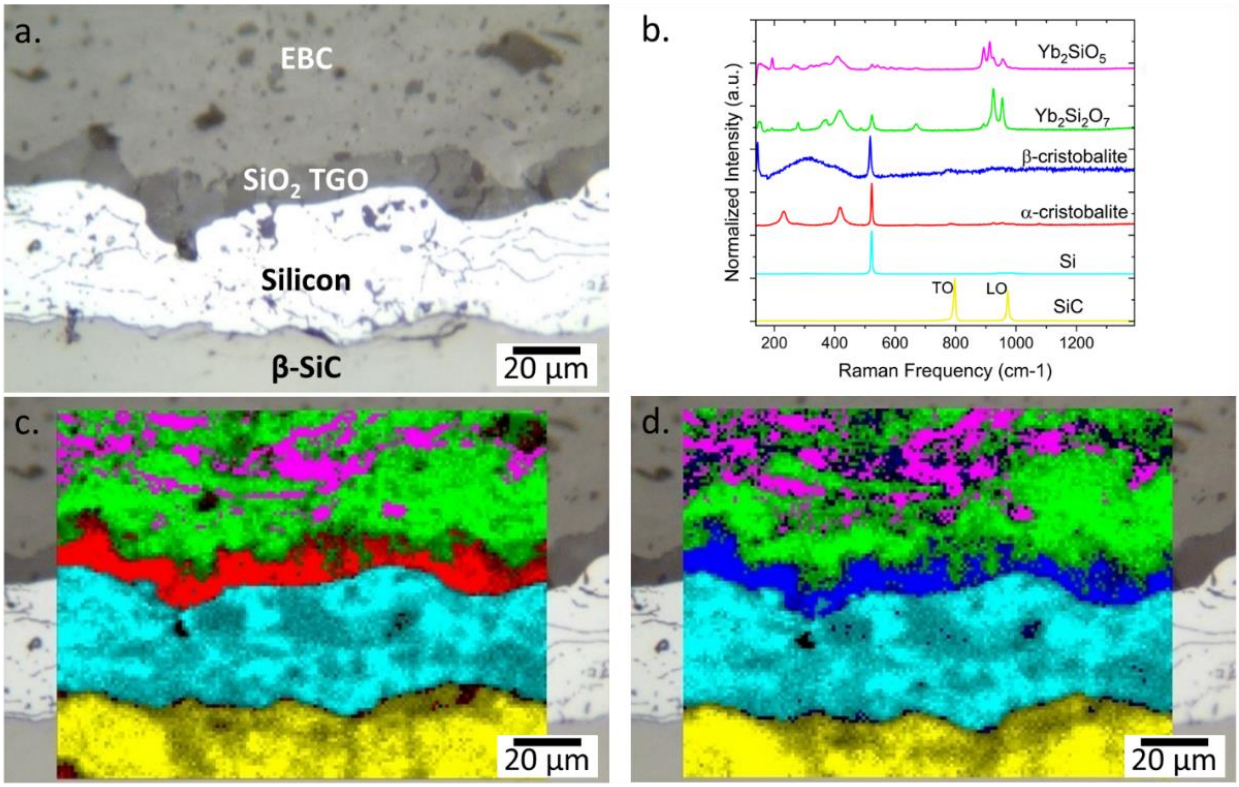

Figure 19. a. Optical image of an EBC cross-section after steam exposure at 1350°C for 1000h, b. Raman spectra for each layer component, c. Raman mapping at 260°C, and d. Raman mapping at 270°C.

2D finite element modeling showed the SiO_2 phase transformation as the dominant source of stress in the EBC system during thermal cycling. Additionally, the model allowed for an understanding of the EBC stress. Figure 20 shows the global EBC stress upon cooling from 1350°C to room temperature. Columns 1, 2, and 3 differentiate difference EBC/SiC architectures, where column 2 most closely represents the current architecture for test samples: EBC/SiO_2/Si bond coating/SiC CMC. From Figure 20, the EBC stress became more compressive with increasing SiO_2 thickness underneath the EBC. In light of this finding, Raman spectroscopy was utilized to measure the global EBC stress after thermal cycling in steam. Photo-Stimulated Luminescence Spectroscopy (PSLS) allows for measurements of the luminescence spectra from dopants [10] and was utilized here. In this instance, a doped EBC was used as the dopants show large luminescence peaks in the red spectrum, Figure 21.

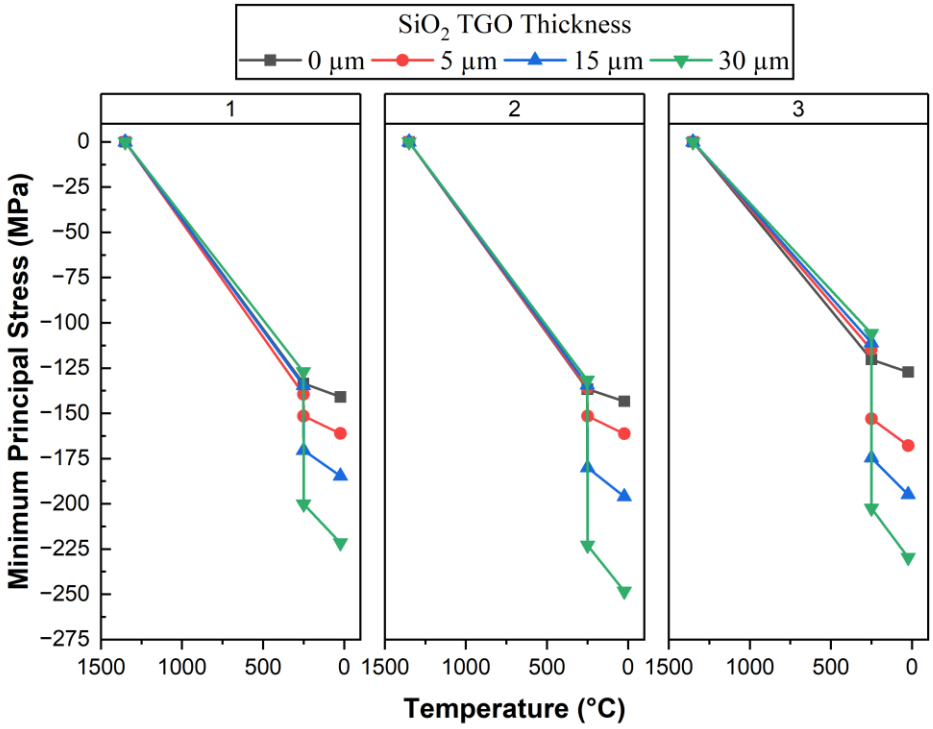

Figure 20. EBC compressive stress through the silica phase change from initial FEM.

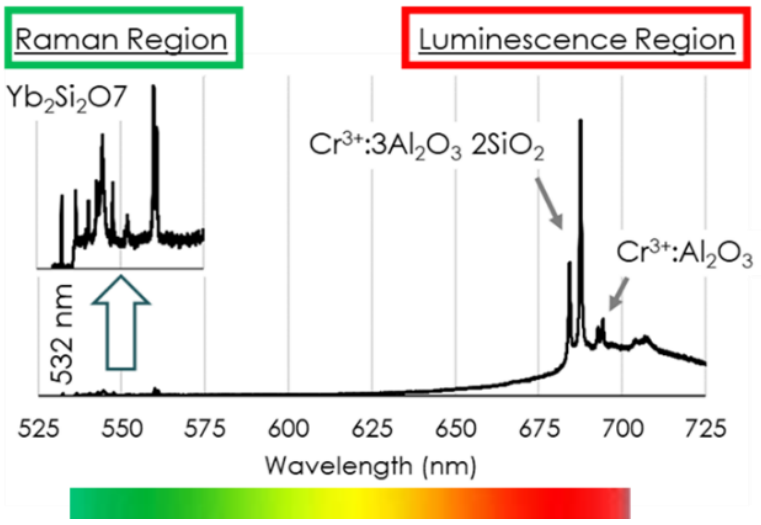

Figure 21. Raman spectra for GRC+D3 EBC chemistry.

The EBC was characterized in the as-received state, and after 100, 300, and 500 h of exposure at 1350°C in Figure 22. The as-received state was primarily amorphous, resulting in a lower peak position. As such, peak shifting from the as received to the 100-h exposure sample was likely related to the crystallization behavior and not solely due to the stress imparted by SiO_2 growth. The peak shifting can be correlated to stress, by setting the 100-h exposure sample as the zero-stress reference. From the zero-stress reference, there is a clear increase in compressive stress for the EBC. Additionally, the stress magnitudes agree with the simplified 2D finite element model results, Table 2. This work validates the simplified finite element, and suggests

that the growth of the EBC, in addition to thermal cycling, results in an increase in stress buildup within the EBC. Such information will be used to identify a critical stress state for EBC failure, in support of future iterations of the EBC lifetime model.

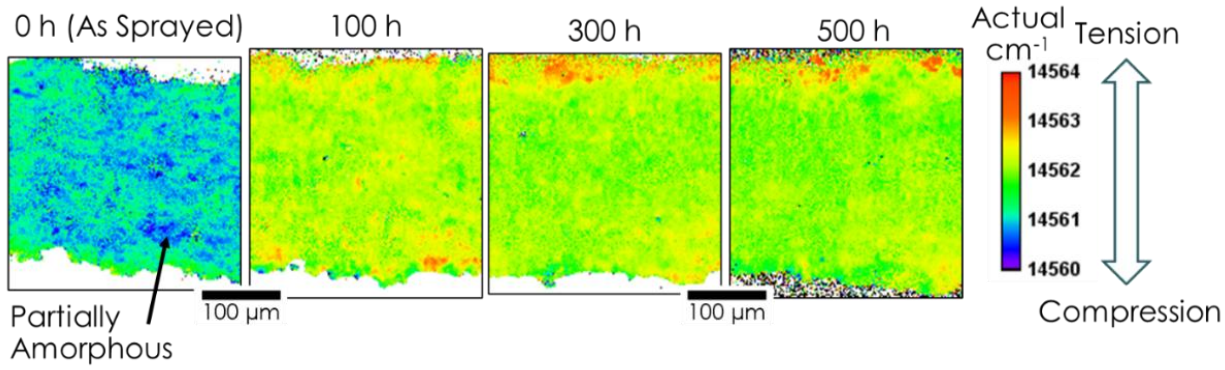

Figure 22. PSLS peak shifting for YbDS+D3 EBC after steam thermal cycle testing up to 500 h.

Table 2. Average EBC stress after thermal cycling.

Average EBC Stress (MPa)	
2D FEM, Calculated	PSLS, Measured
0	0
-8	-13
-15	-17

5. SUMMARY

Considerable progress was made during this project in improving understanding of EBC performance. Experiments measured reaction rates and CTE values as inputs for the EBC lifetime model. As part of that process, a methodology was developed to make 1000's of measurements of the SiO_2 TGO and a framework was quantified to assess EBC performance. The lifetime model was established for thermal cycle performance in flowing steam and was validated across a wide temperature range. The model can be further improved with additional kinetic data and improved temperature dependent properties with additional testing. Further, pressure, velocity, and thermal gradient effects need to be implemented to better simulate real world combustion environments. In addition, the next project will measure O diffusivity through EBCs to refine the model. An overall focus will be refining the EBC failure criteria by assessing the current critical scale thickness strategy and exploring other defect-based criteria.

6. PUBLICATIONS

1. Su YF, Stack PIM, Stephens CJ, *et al.* Quantifying High Temperature Corrosion. NACE CORROSION. OnePetro; 2021
2. Kane K, Garcia E, Lance M, Parker C, Sampath S, Pint B. Accelerated oxidation during 1350°C cycling of ytterbium silicate environmental barrier coatings. *J Am Ceram Soc.* 2021;105(4):2754–2763. https://doi.org/10.1111/jace.18231
3. Kane K, Garcia E, Stack P, *et al.* Evaluating steam oxidation kinetics of environmental barrier coatings. *J Am Ceram Soc*. 2022;105(1):590–605. https://doi.org/10.1111/jace.18093
4. Stack P, Kane KA, Sweet M, *et al.* Dry air cyclic oxidation of mixed Y/Yb disilicate environmental barrier coatings and bare silica formers. *J Eur Ceram Soc*. 2022. https://doi.org/10.1016/j.jeurceramsoc.2022.02.009
5. Ridley M, Kane K, Lance M, *et al.* Steam oxidation and microstructural evolution of rare earth silicate environmental barrier coatings. *J Am Ceram Soc*. 2023;106(1):613–620. https://doi.org/10.1111/jace.18769
6. Kane KA, Garcia E, Uwanyuze S, *et al.* Steam oxidation of ytterbium disilicate environmental barrier coatings with and without a silicon bond coat. *J Am Ceram Soc.* 2021;104(5):2285–2300. https://doi.org/10.1111/jace.17650
7. Ridley M, Garcia E, Kane K, Sampath S, Pint B. Environmental barrier coatings on enhanced roughness SiC: Effect of plasma spraying conditions on properties and performance. *J Eur Ceram Soc*. 2023;43(14):6473–6481. https://doi.org/10.1016/j.jeurceramsoc.2023.06.049
8. Pint BA, Stack P, Kane KA. Predicting EBC Temperature Limits for Industrial Gas Turbines. *Vol. 6 Ceram. Ceram. Compos. Coal Biomass Hydrog. Altern. Fuels Microturbines Turbochargers Small Turbomachines*. Virtual, Online: American Society of Mechanical Engineers; 2021:V006T02A005. https://doi.org/10.1115/GT2021-59408
9. Lance MJ, Ridley MJ, Kane KA, Pint BA. Raman spectroscopic characterization of SiO2 phase transformation and Si substrate stress relevant to EBC performance. *J Am Ceram Soc*. 2023;106(10):6205–6210. https://doi.org/10.1111/jace.19190
10. Lance MJ, Kane KA, Pint BA. The Effect of APS-HVOF Bond Coating Thickness Ratio on TBC Furnace Cycle Lifetime. *Oxid Met*. 2022;98(3):385–397. https://doi.org/10.1007/s11085-022-10127-1